Influence of Biomass Accumulation on Bed Expansion Characteristics of a Down-Flow Anaerobic Fluidized-Bed Reactor

D. García-Calderón,[1] P. Buffière,[1] R. Moletta,[1] S. Elmaleh[2]

[1]Laboratoire de Biotechnologie de l'Environnement INRA, Avenue des Etangs 11100 Narbonne, France; telephone: (33) 468425176; fax: (33) 468425160; e-mail: garcia@ensam.inra.fr
[2]Groupe Génie des Procédés, Université Montpellier II, CC 024 34095 Montpellier Cedex 5, France

Received 20 February 1997; accepted 20 June 1997

Abstract: This article describes the bed expansion characteristics of a down-flow anaerobic fluidized bed reactor treating a synthetic wastewater. Experiments were carried out in a 0.08 m diameter and 1 m length PVC column. The carrier used was ground perlite (an expanded volcanic rock). Particles characteristics were 0.968 mm in diameter, specific density of 213 kg · m^{-3} and U_{mf} (minimal fluidization velocity): 2.3 m · h^{-1}. Experimental data of terminal velocities and bed expansion parameters at several biofilm thicknesses were compared to different models predicting the bed expansion of up-flow and down-flow fluidized beds.

Measured bed porosities at different liquid superficial velocities for the different biofilm thicknesses were in agreement with the Richardson-Zaki model, when U_t (particle terminal velocity) and n (expansion coefficient) were calculated by linear regression of the experimental data. Terminal velocities of particles at different biofilm thicknesses calculated from experimental bed expansion data, were found to be much smaller than those obtained when C_d (drag coefficient) is determined from the standard drag curve (Lapple and Sheperd, 1940) or with others' correlations (Karamanev and Nikolov, 1992a,b). This difference could be explained by the fact that free-rising particles do not obey Newton's law for free-settling, as proposed by Karamanev and Nikolov (1992a,b) and Karamanev et al. (1996). In the present study, the same free-rising behavior was observed for all particles (densities between 213 and 490 kg · m^{-3}). *Biotechnol Bioeng* **57:** 136–144, 1998.
Keywords: down-flow fluidization; bed expansion; biofilm

INTRODUCTION

Fluidized-bed technology has been applied successfully the last few decades to wastewater treatment, both aerobic and anaerobic (Heijnen et al., 1989; Sutton, 1980). In anaerobic digestion, the fluidized-bed technology allows for a higher reactor biomass hold-up than in other anaerobic configurations. Therefore, it is possible to work at high organic loading rates and short hydraulic retention times.

The term *fluidization,* is usually associated with two-or three-phase systems, in which solid particles are fluidized by a liquid or gas stream flowing in the opposite direction of gravity. In the classic case of fluidized systems, the solid particles have a higher density than the fluid. In down-flow (or inverse) fluidization, the liquid specific density is higher than the particle specific density, and the bed is expanded downward by the liquid flow (Karamanev and Nikolov, 1992a).

Down-flow fluidization was recognized first in the early 70's (Ibrahim et al., 1996), but it has received less attention than up-flow fluidization. A number of workers have studied the hydrodynamics of the inverse fluidized bed with non-biological particles (Chern et al., 1982; Fan et al., 1982a,b; Hihn, 1992; Ibrahim et al., 1996; Karamanev and Nikolov, 1992a,b; Karamanev et al., 1996; Legile et al., 1988), but there is a lack of information concerning bed-expansion characteristics of down-flow fluidized beds with attached microbial growth.

The natural process of biomass accumulation may provoke important changes in the down-flow fluidized bed of particles: The growth of biofilm on the surface enlarges particle diameter. It also increases particle specific density, because wet density of the biofilm is higher than the specific density of the carrier material. Thus, there is an increase of the bed expansion at the same fluidization velocity. This phenomenon has to be considered in order to control the expansion of the bed and the OLR (Organic Loading Rate) in anaerobic digestion processes.

Bed Expansion Models for Free-Settling Particles

Like the anaerobic up-flow fluidized bed reactor, the anaerobic down-flow fluidized-bed reactor can be studied as a classic solid-liquid fluidized bed, because there are no reports of substantial effect of gas production on bed expan-

Correspondence to: Diana García-Calderón

 CCC 0006-3592/98/020136-09

sion (Diez-Blanco et al., 1995; Setiadi, 1995) at low OLR. Thus, the relationship between bed expansion and superficial liquid velocity can be described with the models presented by Garside and Al-Dibouni (1977) and classified by Fan et al. (1982a) in three main groups:

- Group 1: Correlations expressing dependence between U_l/U_i and ϵ. Those are the most popular models, such as the Richardson-Zaki model (Richardson and Zaki, 1954).
- Group 2: Bed expansion correlations utilizing the drag force function for a multiparticle system, expressed in terms of the Archimedes number (Ar) and Reynolds number (Re).
- Group 3: Bed expansion is correlated to the main variables of the system, such as particle diameter and density, and liquid velocity.

Among all these models, one of the most popular is the Richardson and Zaki model:

$$\epsilon^n = \frac{U_l}{U_i} \tag{1}$$

The expansion index (n) is a function of the particle terminal Reynolds number Re_t and the relationship between the particle diameter and the column diameter. It can be calculated from the next correlations:

$$n = \left(4.4 + 18\frac{d_p}{D}\right) Re_t^{-0.1} \quad \text{for } 1 < Re_t < 200 \tag{1a}$$

$$n = 4.4\, Re_t^{-0.1} \quad \text{for } 200 < Re_t < 500 \tag{1b}$$

$$n = 2.4 \quad \text{for } Re_t > 500 \tag{1c}$$

U_i can be calculated from the next equation:

$$\log U_i = \log U_t - \frac{d_p}{D} \tag{2}$$

where U_t is determined as follows (Sakiadis, 1984):

$$U_t = \sqrt{\frac{4(\rho_l - \rho_m)g d_p}{3\rho_l C_d}} \tag{3}$$

C_d is the drag coefficient, that has been found to be a function of the shape of the particle and the Reynolds number. For spherical rigid particles, it can be determined from the plot of drag coefficient vs. Re (Sakiadis, 1984):

$$C_d = 24/Re \quad \text{For } Re < 0.1 \tag{4a}$$

$$C_d = (24/Re)(1 + 0.14\, Re^{0.70}) \quad \text{For } Re < 1{,}000 \tag{4b}$$

$$C_d = 0.445 \quad \text{For } 1000 < Re < 350{,}000 \tag{4c}$$

$$C_d = 0.19 - [(8)(10^4)/Re] \quad \text{For } Re > 10^6 \tag{4d}$$

Where Re is determined from:

$$Re = \frac{U\rho_l d_p}{\mu_l} \tag{5}$$

Several authors have studied the bed expansion characteristics of up-flow fluidized particles with attached microbial growth. Ngian and Martin (1980), Hermanowicz and Ganczarczyk (1983) and Mulcahy and Shieh (1987) have compared experimental expansion data from fluidized biological beds to values obtained with the Richardson and Zaki model. All these authors agree with the fact that this correlation can be applied only with some restrictions to fluidized beds with biocoated particles.

Ngian and Martin (1980) observed that the Richardson-Zaki correlation gave a satisfactory estimate of U_t only for small particles (0.61 mm diameter). For larger particles (1.55 mm diameter) the predicted U_t was found to be 30 to 70% below the experimentally determined U_t.

Hermanowicz and Ganczarczyk (1983) and Mulcahy and Shieh (1987) observed a difference between experimental and calculated U_t from Equation (3). They concluded that this difference is due to the drag coefficient (C_d). Both studies proposed a modified formula for the drag coefficient in order to use the Richardson-Zaki model for calculation of the expansion of an up-flow fluidized bed with bioparticles:

$$C_d = 17.1\, Re_t^{-0.47}$$

Hermanowicz and Ganczarczyk (1983), (nitrifying bioparticles) and

$$C_d = 36.66 Re_t^{-\frac{2}{3}} \tag{7}$$

Mulcahy and Shieh (1987), (denitrifying bioparticles).

Free-Rising Particles

The Richardson Zaki model, as well as the other bed expansion correlations are made for up-flow fluidized beds, with free-settling particles. Only a few correlations have been proposed for down-flow fluidized-bed expansion. There are the two empirical correlations proposed by Fan et al. (1982a). The first is based on the group 1 models:

$$\epsilon^n = \frac{U_l}{U_i} \tag{8}$$

where:

$$n = 15 Re_t^{-0.35} e^{3.9\frac{d_p}{D}} \quad \text{for } 350 < Re_t < 1250 \tag{9a}$$

$$n = 8.6 Re_t^{-0.2} e^{-0.75\frac{d_p}{D}} \quad \text{for } Re_t > 1250 \tag{9b}$$

The second one is based on the group 2 models:

$$f = 3.21\epsilon^{-4.05} Ar^{-0.007} e^{3.5\frac{d_p}{D}} \tag{10}$$

where:

$$f = Ar/13.9Re^{1.4} \quad \text{for } 2 < Re < 500 \tag{11a}$$

$$f = 3Ar/Re^2 \quad \text{for } Re > 500 \tag{11b}$$

Ar is the Archimedes number:

$$\mathrm{Ar} = \frac{d_p^3(\rho_l - \rho_m)\rho_l g}{\mu_l^2} \tag{12}$$

Recently, Karamanev and Nikolov (1992a,b) and Karamanev et al. (1996), after an extensive work, found that free-rising particles do not obey free-settling laws. They studied the rising trajectories of several light particles with different specific densities and diameters, and their studies showed the unusual behavior of the inverse fluidized bed. They observed that the standard drag curve (from Lapple and Sheperd, 1940) is not valid for rising spheres with a density below 300 $kg \cdot m^{-3}$.

Karamanev and Nikolov (1992a,b) proposed that the drag coefficient of free-rising particles is a constant, equal to 0.95 for $\rho_m < 300\ kg \cdot m^{-3}$ and $Re_t > 130$. For $Re_t < 130$ and/or $\rho_m > 900\ kg \cdot m^{-3}$, C_d can be described by the laws of free-settling. They determined C_d with the correlation of Turton and Levenspiel (1986):

$$C_d = \frac{24(1 + 0.173\ \mathrm{Re}_t^{0.657})}{\mathrm{Re}_t} + \frac{0.413}{1 + 16{,}300\ \mathrm{Re}_t^{-1.09}} \tag{13}$$

Karamanev et al. (1996) proposed two regimes for the free rise of light spheres. The first one, observed when $Re/d_p < 1450$ is characterized by a rectilinear motion of the solid sphere, and C_d follows the standard curve. The second one is observed when $Re/d_p > 1450$. The C_d is constant and equal to 0.95 and the sphere follows a spiral trajectory.

The aim of this work is to compare the experimental bed expansion data of an anaerobic down-flow fluidized bed reactor at different biofilm thicknesses to different bed expansion models, for both up-flow and down-flow fluidized beds.

MATERIALS AND METHODS

Physical Properties of Carrier

The carrier material was ground perlite, an expanded volcanic rock. Commercially available perlite was ground in a Dietz Mühle grinder and sieved (mesh size 0.7–1 mm). It was calcinated to eliminate impurities, and then washed. Settled fraction was eliminated. Shape and size of particles were determined by microscopic observations (Olympus CH-2 microscope, 2 mm Leitz-Wetzler slide with 0.01 mm intervals). Average particle diameter was calculated by Sauter's mean diameter method for a sample of 80 particles. Apparent specific density was considered as the weight of 1 L of the material. Minimum fluidization velocity was calculated by the correlation of pressure-drop experimental data at different fluidization velocities.

Specific dry density was calculated by taking the height of the bed at minimum fluidization:

$$\rho_s = \frac{W}{H_{mf} A(1 - \epsilon_{mf})} \tag{14}$$

Specific wet density was determined as the specific density, taking the mass of wet particles. Table I presents the physical properties of perlite particles.

Experimental Set-Up

The reactor consisted of a PVC column with a conic bottom of a total volume of 5 L including conical bottom (0.08 m diameter, 1 m height). The flow distributor and the gas outlet were placed at the removable cap covering the top section. The gas outlet was connected to a gas meter. Effluent was discharged through a port on the low part of the column, connected to an outlet tube that kept the liquid level in the reactor (see Fig. 1). Recycling was ensured by means of a peristaltic pump (Masterflex Cole Parmer). The reactor temperature was kept constant at 35°C by a water jacket. Figure 1 shows a schematic diagram of the experimental set-up.

Operation Conditions

The anaerobic reactor was inoculated with sludge from an anaerobic pond treating a red wine distillery wastewater. During the start-up period, the reactor was fed with this wastewater. Then, a synthetic wastewater was used in order to obtain a better control of the inlet concentration (C_{in}). The synthetic wastewater consisted of a mixture of glucose, inorganic salts, and nutrients (composition is given in Table II). Anaerobic conditions were obtained by bubbling nitrogen. To maintain the reactor pH between 6.5 and 7, NaOH was added when needed.

The bed (1.15 L original volume) was expanded at 33%, at a superficial liquid velocity of 8.64 $m \cdot h^{-1}$. The reactor was monitored for temperature, flow rate, pH, gas production, and composition. Attached total solids (TS), attached volatile solids (VS), volatile fatty acids (VFA) and total organic carbon (TOC) were routinely analyzed. After the start-up period, organic loading rate (OLR) was increased stepwise from 3.27 to 5.75 $kg \cdot m^{-3} \cdot d^{-1}$, by reducing hy-

Table I. Physical characteristics of the carrier (perlite).

Mean diameter (mm)	Specific dry density ($kg \cdot m^{-3}$)	Specific wet density ($kg \cdot m^{-3}$)	Specific area ($m^2 \cdot m^{-3}$)	U_{mf} ($m \cdot h^{-1}$)	Shape
0.968	213	280	6980	2.3	irregular, rough surface

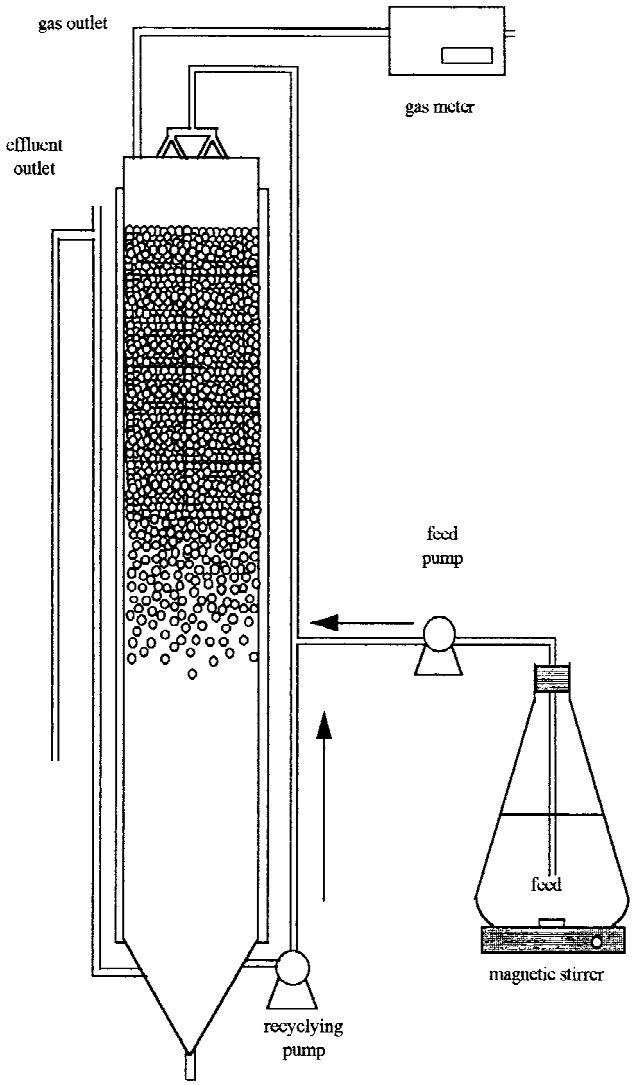

Figure 1. Schematic diagram of the experimental set-up.

draulic retention time (HRT) from 1.35 to 0.87 d. The OLR and HRT were calculated as:

$$OLR = \frac{(Q_{in})(C_{in})}{(V_{\exp})(\epsilon)} \tag{15}$$

$$HRT = \frac{(V_{\exp})(\epsilon)}{Q_{in}} \tag{16}$$

Corrections were made because of the bed expansion which was due to biomass hold-up in time.

Bioparticles and Bed Expansion

Bioparticles samples were withdrawn from three sampling points in the reactor. Biomass development was monitored by taking biocovered particle samples and determining the total attached VS. It was considered that attached VS corresponded to the biomass weight.

Table II. Synthetic feed composition.

Substrate	(mg · L^{-1})	Oligoelements solution	(mg · L^{-1})
Glucose	12500	$FeCl_3 \cdot 6H_2O$	1500
Yeast extract	50	H_3BO_3	150
Peptone	50	$CuSO_4 \cdot 5H_2O$	30
NH_4Cl	38	KI	30
$MgSO_4 \cdot 7H_2O$	600	$MnCl_2 \cdot 4H_2O$	120
$CaCl_2 \cdot H_2O$	70	$NaMoO_4 \cdot 2H_2O$	60
EDTA	100	$ZnSO_4 \cdot 7H_2O$	120
KH_2PO_4	1361.7	$CoCl_2 \cdot 6H_2O$	150
K_2HPO_4	7125.6		
Oligoelements solution	2 ml · L^{-1}		

Bioparticle diameters were calculated according to Setiadi (1995):

$$d_b = \sqrt[3]{\frac{d_p^3(1-\epsilon)}{\left(\frac{W}{\rho_b HA}\right)}} \tag{17}$$

Biofilm thickness was determined according to Shieh et al. (1981):

$$d_b = d_p + 2\sigma \tag{18}$$

Bioparticle density was calculated according to Shieh et al. (1981):

$$\rho_b = \rho_m\left(\frac{d_p}{d_b}\right)^3 + \rho_{bw}\left[1 - \left(\frac{d_p}{d_b}\right)^3\right] \tag{19}$$

where ρ_{bw} is considered as 1000 kg · m^{-3}.

For each biofilm thickness, the influence of superficial liquid velocity on bed expansion was investigated.

Bed voidage was calculated in terms of expanded bed height, according to the next equation:

$$\epsilon = 1 - \frac{H_{mf}(1-\epsilon_{mf})}{H} \tag{20}$$

with $\epsilon_{mf} = 0.4$.

Measured U_t

Terminal particle velocity for clean perlite and biocovered particles were determined experimentally by releasing particles in a column of 0.05 m diameter filled with water, and recording the traveling time between two marks at a 0.5 m interval.

TS and VS were determined using standard methods (American Public Health Assoc., 1985). pH was measured with a Mettler Toledo 1100 Calimatic pH meter.

RESULTS AND DISCUSSION

Biomass Accumulation

Biomass accumulation was measured by the increase of the attached VS on perlite particles. Samples were taken at three

different heights of the reactor, because it was noticed that particle segregation occurred with time. At the upper part of the fluidized bed, the attached VS concentration was always lower than in the lower levels of the bed. Particles with thicker biofilm were found at the lowest level of the reactor, because particle terminal velocity decreased as biofilm accumulated. Al-Dibouni and Garside (1979) consider particle dispersion in a fluidized bed to be influenced by several parameters: overall porosity, liquid superficial velocity, particle size, density, and shape.

Figure 2 shows the biofilm development (average of the three sample points), as well as the particle density and diameter at the different biofilm thicknesses.

The irregular surface of perlite particles allowed an important biomass hold-up. The biomass accumulation modified particle characteristics: The diameter enlarged because of the biofilm thickness and density increased, because biofilm wet density is greater than perlite wet density. Biofilm wet density can be considered equal to 1000 $kg \cdot m^{-3}$, according to Hermanovicz and Ganczarzyk (1983) and Setiadi (1995). Average specific density of biocovered perlite particles increased from 320 to 440 $kg \cdot m^{-3}$ with increasing biofilm thickness from 24 to 61 μm. That means that a biofilm of 37 μm provoked an increase of 38% in the particle density. For up-flow fluidized beds, the biofilm growth results in an inverse phenomenon—the decrease of the particle density because biofilm wet density is lower than the particle density (Hermanovicz and Ganczarzyk, 1983; Ngian and Martin, 1980). Setiadi (1995) observed that for an up-flow anaerobic fluidized-bed reactor a 10 μm biofilm increase leads to a 20% decrease in the density of sand particles.

However, under certains conditions, biofilm density can be as high as 2400 $kg \cdot m^{-3}$, (adhesion of pollution to support particles after its destabilization by ferric or aluminium salts) (Myška and Švec, 1994). In this case, behavior of particles with a heavy biofilm is particularly affected.

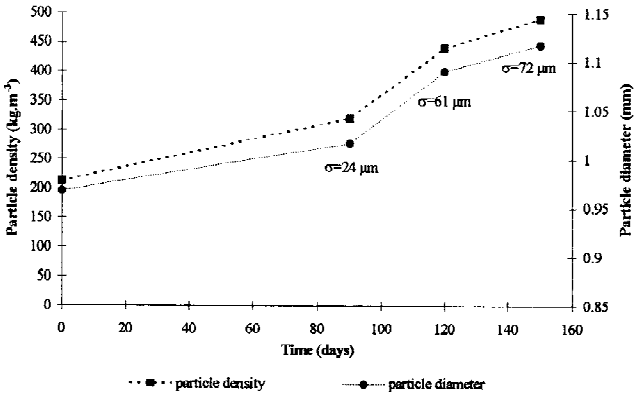

Figure 2. Average biofilm accumulation and particle characteristics at the different biofilm thicknesses (σ). 24 μm = 0.12 g of biomass per g of perlite; 61 μm = 0.16 g of biomass per g of perlite; 72 μm = 0.18 g of biomass per g of perlite.

Bed Expansion at the Different Biofilm Thicknesses

Uncoated particles presented the lowest bed expansion rate. At the same superficial liquid velocity, bed expansion increased as biofilm thickness increased because of two reasons: (1) Biofilm accumulation enlarges particles, and thus, original bed expansion is modified; and (2) U_t decreases as particle density increases (the difference between ρ_l and ρ_m becomes smaller). That means that microbial growth attachment would provoke a greater bed expansion rate at the same fluidization velocity, as has been observed in up-flow fluidized-bed bioreactors (Hermanovicz and Ganczarczyk, 1983; Ngian and Martin, 1980; Ro and Neethling, 1994; Setiadi, 1995).

In this study, no significant influence of biogas production in bed expansion was noticed. This can be due to the fact that at the applied OLR, the gas production rate (it varied from 0.41 to 7.72 $1.1^{-1} \cdot d^{-1}$) was not high enough to disturb the bed hydrodynamics.

Biogas upflow velocity (U_g) was calculated as biogas production divided by reactor section. Because U_g varied between 0.004 and 0.077 $m \cdot h^{-1}$, its influence can be neglected when compared to liquid velocity (U_l), 8.64 $m \cdot h^{-1}$. Several authors (Diez-Blanco et al., 1995; Hermanovicz and Gancarczyk, 1983; Ngian and Martin, 1980; Setiadi, 1995) have studied the influence of liquid velocity on bed expansion in anaerobic/anoxic up-flow fluidized-bed bioreactors. None of them have reported any influence of the gas on the bed-expansion characteristics. Unfortunately, there are no similar experimental data concerning down-flow anaerobic fluidized-bed reactors to make a comparison. Moreover, gas production could provoke some problems at higher biogas production rates, or in bigger reactors. Bed expansion is a very important parameter to control in anaerobic fluidized-bed reactors, because OLR and HRT are calculated with the expanded bed volume.

Comparison of Experimental Data to Richardson-Zaki Model

The plots of U_l vs. ϵ at the different biofilm thicknesses are shown in Figure 3.

As shown, they can be all interpolated by a straight line. By applying linear regression analysis to the data, U_i and n can be determined according to the following form of the equation of the Richardson-Zaki model:

$$lnU_l = lnU_i + nln\epsilon \tag{21}$$

Correlation coefficients for all the biofilm thicknesses were found to be above 0.98. Results are given in Table III. Table III also presents Re_t and C_d determined from experimental data.

From Table III it can be seen that U_t decreased as biofilm became thicker. This is because particles became heavier

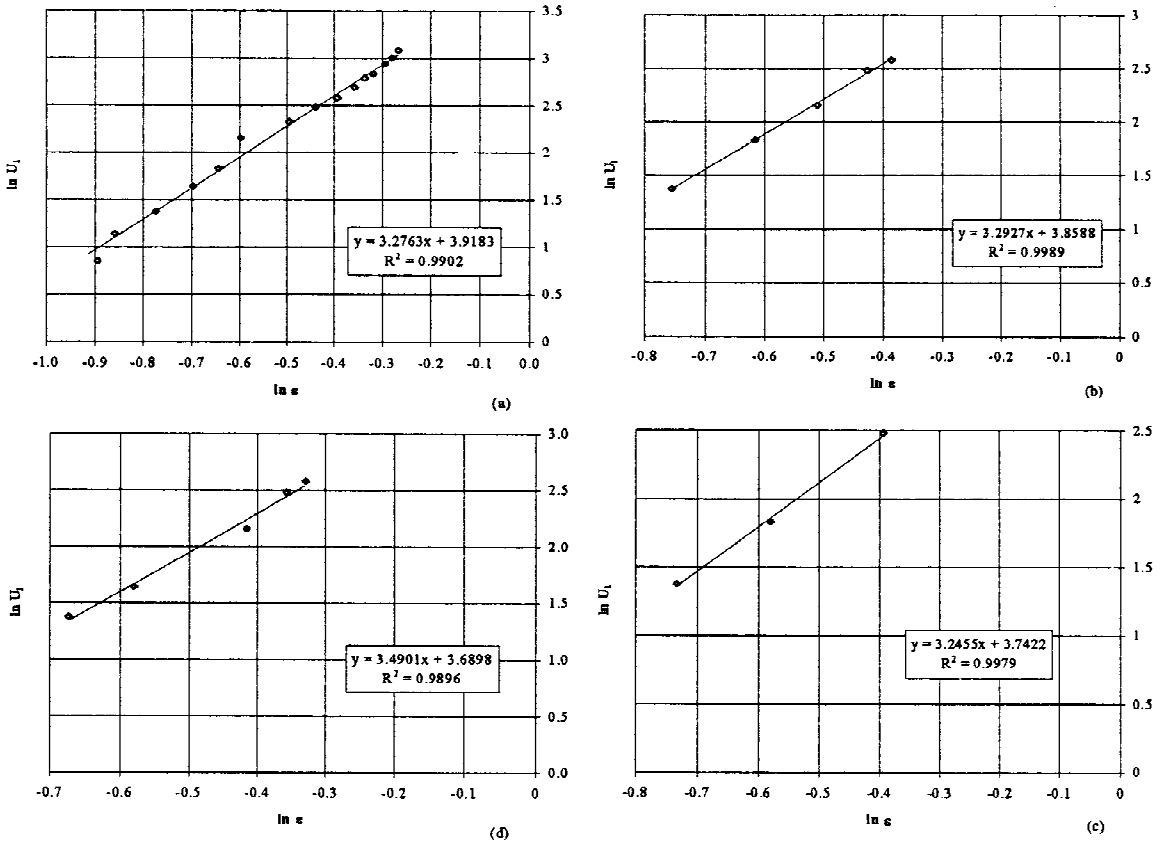

Figure 3. In U_t vs. ln ϵ at the different biofilm thicknesses. (a) 0 μm; (b) 24 μm; (c) 61 μm; (d) 72 μm

with biomass accumulation (their density increases), and thus the difference $\rho_l - \rho_m$ became smaller.

It can also be seen from Table III that there is a great difference between C_d from Equation (3) and C_d from Equation (4). This can be explained by the fact that in Equation (3), C_d is derived directly from experimental U_t values (plot of lnU_l vs. l$n\epsilon$); whereas Equation (4) utilizes the plot of drag coefficient vs. Re (also from experimental U_t). C_d values from Equation (4) thus fit the standard drag curve from Lapple and Sheperd (1940), but if these values are used to calculate U_t with Equation (3) U_t becomes more than 4 times greater. That means that C_d that fit Re_t in the standard drag curve are much smaller than the experimental C_d values.

Garnier et al. (1990) compared the experimental bed-expansion characteristics of an inverse fluidized bed (air-lift bioreactor) to the Richardson-Zaki model. They found that experimental data of three different kinds of polystyrene beads (60, 300, and 400 kg · m^{-3}) fit the Richardson-Zaki model when using U_t 40% smaller than predicted. They explained this fact by the irregular shape of the particles. According to Karamanev and Nikolov (1992a,b) and Karamanev et al. (1996), free-rising particles do not obey the Newton law for free-settling. That means that a free-rising particle and a free-settling particle with the same volume and the same difference between ρ_l and ρ_m have different U_t. They explained this difference by the fact that their trajectories are not the same (rectilinear for free-settling particles and spiral for free-rising particles).

Table III. Bed expansion parameters at the different biofilm thicknesses (experimental U_t).

Biofilm thickness (μm)	Re_t	U_t(m · h^{-1})	n	C_d from Eq. (3)	C_d from Eq. (4)
0	16.8	50.3	3.27	48.64	2.85
24	16.72	47.4	3.29	50.32	2.87
61	15.96	42.2	3.24	57.46	2.95
72	15.52	40	3.49	60.46	3.0

Karamanev and Nikolov (1992a,b) proposed a constant C_d of 0.95 for particles with a density below 300 kg · m^{-3} and Re_t over 130; particles with densities over 900 kg · m^{-3} and/or Re_t below 130 were described by the laws of free-settling. In the present study, all particles behaved differently from free-settling particles. For all the biofilm thicknesses (ρ_m from 213 to 490 kg · m^{-3}), experimental C_d were much higher than the C_d matching the respective Re_t of the standard drag curve.

Because there are no correlations available to predict the bed voidage of a down-flow fluidized bed with bioparticles, it was decided to utilize some correlations proposed for no-biological fluidized-bed systems (up-flow and down-flow) to make a comparison with experimental results.

Table IV. Some theoretical values for the bed expansion parameters at the different biofilm thicknesses.

	Richardson-Zaki, 1954				Nikolov and Karamanev, 1992						
	[C_d from Eq. (4)]				[C_d from Eq. (13)]				(C_d = 0.95)		
Biofilm thickness	C_d	Re_t	U_t ($m \cdot h^{-1}$)	n	U_t ($m \cdot h^{-1}$)	Re_t	C_d	n	U_t ($m \cdot h^{-1}$)	Re_t	n
0 μm	1.21	77.7	231	2.98	143	48.2	1.59	3.21	338	120.4	2.85
24 μm	1.20	78.9	223	2.99	141	49.9	1.56	3.12	351	123.8	2.85
61 μm	1.19	31.2	214	2.99	132	50	1.56	3.13	327	123.8	2.86
72 μm	1.12	85.8	211	2.97	129	52.6	1.51	3.12	318	129.4	2.85

Table IV presents bed expansion parameters determined using: (1) the Richardson-Zaki model, with values of the standard drag curve from Lapple and Sheperd (1940) for C_d and, (2) C_d according to Karamanev and Nikolov (1992b).

It can be seen that in all cases, theoretical values for U_t and Re_t are greater than experimental. This is due to the fact that C_d theoretical values are much smaller than those obtained directly from experimental U_t. In contrast to Karamanev and Nikolov (1992a,b) and Karamanev et al. (1996), it was observed that all particles (densities from 213 to 490 $kg \cdot m^{-3}$) presented C_d that did not fit the standard drag curve. This could be due to the perlite particles which are not homogenous because of the process of expansion. They present crevices and pores, and thus density could vary inside the particle. Indeed, that was observed when U_t was measured.

Nevertheless, a similar phenomenon has been observed in up-flow fluidized-bed bioreactors. Several authors (Ngian and Martin, 1980; Ro and Neethling, 1994; Setiadi, 1995) have observed that in up-flow fluidized bed reactors with microbial growth, experimental data do not fit correlation predictions or if so, then only under certain conditions.

Observed bed voidage for all biofilm thicknesses were compared to some correlations. Figure 4 shows the plots of ϵ vs. U_l for the experimental and predicted bed voidage. All predicted values for bed voidage were lower than those observed. This is the result of the use of a C_d that is not determined directly from experimental U_t. It can be seen that overall bed voidage remains almost constant for all biofilm thicknesses. That means that biomass accumulation does not have an important influence over the overall bed expansion. This could be explained by biomass accumula-

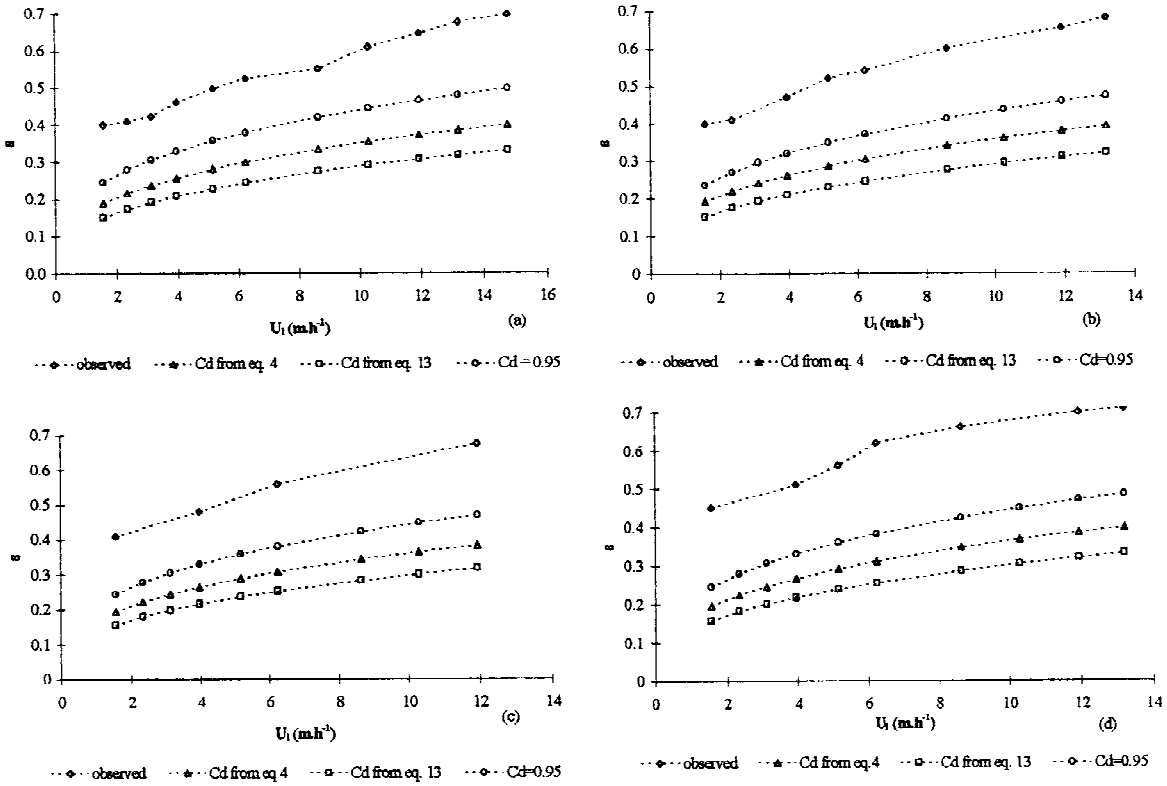

Figure 4. Comparison of experimental results and predicted bed voidage with several correlations. (a) 0 μm; (b) 24 μm; (c) 61 μm; (d) 72 μm.

tion which increases particle volume, but the whole volume of the bed is also increased. Setiadi (1995) observed the same phenomenon for an up-flow fluidized bed bioreactor.

Unfortunately, it is not possible to establish a model predicting C_d for free-rising particles with microbial growth because results of the present study are insufficient. Indeed, it would be necessary to study particles with the widest range of size and density, in order to obtain information for a widest range of Re.

Measured U_t

In order to compare U_t determined from the linear regression analysis of the experimental data (called ''experimental U_t''), it was decided to measure directly U_t as explained in the experimental section. Nevertheless, it was observed that U_t varied a lot for particles with the same overall density. The average U_t were 65 $m \cdot h^{-1}$ for uncoated particles and 27 $m \cdot h^{-1}$ for 72 μm biofilm particles.

This wide range of U_t can be explained by the fact that perlite particles are not homogeneous in density, and they present an irregular shape. This is why we decided to work with U_t derived from the experimental bed expansion study rather than measured U_t, it is more representative of the whole bed.

CONCLUSIONS

The present study compared experimental data from a down-flow fluidized-bed bioreactor to some correlations predicting bed expansion of both up-flow and down-flow fluidized beds.

Results showed that free-rising spheres do not obey Newton's law for free-settling, as proposed by Karamanev and Nikolov (1992a,b) and Karamanev et al. (1996). Nevertheless, in this study all particles (densities between 213 and 490 $kg \cdot m^{-3}$) presented experimental U_t values much smaller than predicted. This could be due to the fact that C_d for free-rising particles is greater than that for free-settling particles because of the particle trajectory (as proposed by the previously cited authors), and to the fact that perlite particles are irregular and not homogeneous due to the process of expansion.

A further study should be done in order to determine a model describing the bed expansion of free-rising particles with biomass.

NOMENCLATURE

n	expansion index (dimensionless)
V_{exp}	expanded bed volume (m^3)
W	mass of clean particles (kg)
d_p	particle diameter (mm)
d_b	bioparticle diameter (mm)
C_d	drag coefficient (dimensionless)
Ar	Archimedes number (dimensionless)
Re	Reynolds number (dimensionless)
Re_t	terminal particle Re (dimensionless)
U_1	superficial liquid velocity ($m \cdot h^{-1}$)
U_t	terminal particle velocity ($m \cdot h^{-1}$)
U_{mf}	minimum fluidization velocity ($m \cdot h^{-1}$)
U_g	superficial gas velocity ($m \cdot h^{-1}$)
A	sectional area (m^2)
D	column diameter (m)
H	bed height (m)
H_{mf}	bed height at minimum fluidization (m)
HRT	hydraulic retention time (days)
OLR	organic loading rate ($kg\ TOC \cdot m^{-3} \cdot d^{-1}$)
Q_{in}	inlet flow rate ($m^{-3} \cdot d^{-1}$)
C_{in}	TOC inlet ($kg\ TOC \cdot m^{-3}$)
TOC	total organic carbon ($kg \cdot m^{-3}$)
TS	Total solids ($g \cdot l^{-1}$)
VS	volatile solids ($g \cdot l^{-1}$)

Greek symbols

μ_1	liquid viscosity ($kg \cdot m^{-1} \cdot S^{-1}$)
ρ_l	liquid specific density ($kg \cdot m^{-3}$)
ρ_m	solid specific density ($kg \cdot m^{-3}$)
ρbw	biofilm wet density ($kg \cdot m^{-3}$)
σ	biofilm thickness (μm)
ϵ	bed voidage (dimensionless)
ϵ_{mf}	bed voidage at minimum fluidization (dimensionless)

References

Al-Dibouni, M. R., Garside, J. 1979. Particle mixing and classification in liquid fluidized beds. Trans. Int. Chemical Engrs. **57**: 94–103.

Chern, S., Muroyama, K., Fan, L. 1982. Hydrodynamic considerations of constrained inverse fluidization and semifluidization in a gas-liquid-solid system. Chem. Eng. Sci. **38**: 1167–1174.

Davison, B. H. 1988. Dispersion and hold-up in a three-phase fluidized bed bioreactor. Proceedings 10th Symposium on Biotechnology for Fuels and Chemicals, Gatlinburg, Tennessee.

Diez-Blanco, V., Garcia-Encina, P. A., Fernández-Polanco, F. 1995. Effect of biofilm growth, gas and liquid velocities on the expansion of an anaerobic fluidized bed reactor (AFBR). Wat. Res. **29**: 1649–1654.

Fan, L., Muroyama, K., Chern, S. 1982a. Hydrodynamic characteristics of inverse fluidization in liquid-solid and gas-liquid-solid systems. Chem. Eng. J. **24**: 143–150.

Fan, L., Muroyama, K., Chern, S. 1982b. Some remarks on hydrodynamics of inverse fluidization in gas-liquid-solid systems. Chem. Eng. J. **3**: 1570–1572.

Garnier, A., Chavarie, C., André, G., Klvana, D. 1990. The inverse fluidization airlift bioreactor, part I: Hydrodynamic studies. Chem. Eng. Comm. **98**: 31–45.

Garside, J., Al-Duboni, M. R. 1977. Velocity-voidage relationships for fluidization and sedimentation in solid-liquid systems. Ind. Eng. Chem. Process Des. Dev. **16**: 206–214.

Heijnen, J. J., Mulder A., Enger, W., Hoeks, F. 1989. Review on the application of anaerobic fluidized bed reactors in wastewater treatment. Chem. Eng. J. **41**: B37–B50.

Hermanovicz, S. W., Ganczarczyk, J. J. 1983. Some fluidization characteristics of biological beds. Biotechnol. Bioeng. **25**: 1321–1330.

Hihn, J. 1992. Contribution à l'étude d'un lit fluidisé triphasique inverse fonctionnant à contre-courant: Hydrodynamique et transfert de matière gaz/liquide. Ph.D. thesis, ESIGEC, University of Savoie, Chambéry, France.

Ibrahim, Y. A., Briens, C. L., Margaritis, A., Bergongnou, M. A. 1996. Hydrodynamic characteristics of a three-phase inverse fluidized bed column. AlChE Jour. **42**: 1889–1900.

Karamanev, D. G., Nikolov, L. N. 1992a. Free-rising spheres do not obey Newton's law for free-settling. AlChE Jour. **38**: 1843–1846.

Karamanev, D. G., Nikolov, L. N. 1992b. Bed expansion of liquid-solid inverse fluidization. AlChE Jour. **38**: 1916–1922.

Karamanev, D. G., Chavarie, C., Mayer, R. C. 1996. Dynamics of the free rise of a light sphere in liquid. AlChE Jour. **42**: 1789–1792.

Lapple, C. E., Sheperd, C. B. 1940. Calculation of particle trajectories. Industrial and Engineering Chemistry. **35**: 605–617.

Legile, P., Menard, G., Laurent, C., Thomas, D., Bernis, A. 1988. Contribution à l'étude hydrodynamique d'un lit fluidisé triphasique inverse fonctionnant à contre-courant. Entropie **143–144**: 23–31.

Mulcahy, L. T., Shieh, W. K. 1987. Fluidization and reactor biomass characteristics of the denitrification fluidized bed reactor. Wat. Res. **21**: 451–458.

Myška, J., Švec, J. 1994. The distributive properties of a fluidized bed with biomass. Wat. Res. **28**: 1653–1658.

Ngian, K., Martin, W. R. B. 1980. Bed expansion characteristics of liquid fluidized bed particles with attached microbial growth. Biotechnol. Bioeng. **22**: 1843–1856.

Richardson, J. F., Zaki, W. N. 1954. Sedimentation and fluidization: Part 1. Trans. Instn. Chem. Engrs. **32**: 35–53.

Ro, K. S., Neethling, J. B. 1994. Biological fluidized beds containing widely different bioparticles. J. Environ. Engin. **120**: 1416–1426.

Sakiadis, B. C. 1984. Fluid and particle mechanics. pp. 563–565 In: D. W. Green and J. O. Maloney (eds.), Perry's chemical engineer's handbook, 6th edition. Mc Graw Hill, New York.

Setiadi, T. 1995. Predicting the bed expansion of an anaerobic fluidized-bed bioreactor. Wat. Sci. Tech. **31**: 181–191.

Shieh, W. K., Sutton, P. M., Kos, P. 1981. Predicting reactor biomass concentration in a fluidized bed system. JWPCF. **53**: 1574–1584.

16th edition. American Public Health Association. 1985. Standard methods for the examination of water and wastewater. Washington, DC.

Sutton, P. M. 1980. Application of the oxytron system™ fluidized bed process to industrial wastewater treatment. pp. 607–613. In: M. Murray (ed.), Adv. in biotechnol., Vol. II: Fuels, chemicals and waste treatment. Pergamon Press, Oxford, United Kingdom.

Turton, R., Levenspiel, O. 1986. A short note on the drag correlation for spheres. Powder Technol. **47**: 83–86.